Inorganic Chemistry

pubs.acs.org/IC

Article

A Family of Highly Emissive Lanthanide Complexes Constructed with 6-(Diphenylphosphoryl)picolinate

Chen Wei, Boxun Sun, Zifeng Zhao, Zelun Cai, Jiajia Liu, Yu Tan, Huibo Wei,* Zhiwei Liu, Zuqiang Bian,* and Chunhui Huang

Cite This: https://dx.doi.org/10.1021/acs.inorgchem.0c00444

Read Online

ACCESS | Metrics & More | Article Recommendations | Supporting Information

ABSTRACT: We report a novel family of lanthanide complexes $Ln(DPPOP)_3$ (Ln = Pr, Nd, Sm, Eu, Tb, Dy, Er, and Yb) employing anionic tridentate (O^N^O) ligand 6-(diphenylphosphoryl)picolinate (DPPOP). Crystal structures of the complexes reveal that each lanthanide ion is nine-coordinated by three tridentate ligands. In the crystals, 1D channels are found, which can absorb and eliminate water reversibly. DPPOP possesses high triplet energy and can sensitize a series of lanthanide ions. An energy transfer mechanism is proposed through the higher excited states of the lanthanide ions. In the solid state, remarkably high quantum yields in the visible range are obtained: 81% for Eu(III), 97% for Tb(III), 13% for Dy(III), and 4% for Sm(III) complex.

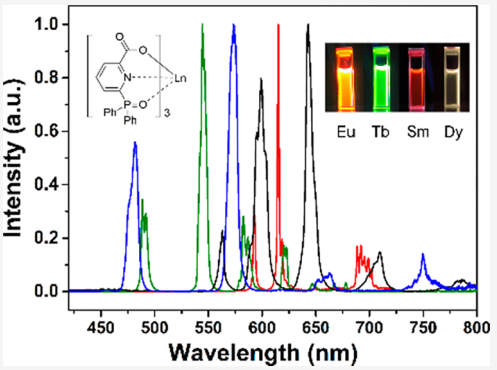

INTRODUCTION

Trivalent lanthanide complexes have been utilized as light-emitting materials in a variety of fields, such as bioimaging,[1] sensing,[2] organic light-emitting diodes,[3] and light conversion for solar cells,[4] due to their unique characters including narrow emission peaks, long luminescence lifetimes, and large Stokes shifts.

To obtain efficient luminescence from lanthanide complexes, the ligands play quite an important role because they not only serve as "antennae" to absorb and transfer energy but also protect the central ions from quenching by the environment. To design an ideal ligand, the following basic issues should be considered: (1) The donor energy level (usually triplet state) of the ligand ensures efficient energy transfer to the lanthanide ion.[5] (2) Quenching pathways including low-lying ligand to metal charge transfer (LMCT) states and vibrations of O−H and N−H groups in the ligand are avoided.[6] (3) Good coordinating stability and a large steric hindrance are present to prohibit the binding of water and other small solvent molecules in the first or second coordination sphere, which bring serious vibrational quenching.

With these considerations, researchers have developed various ligands to coordinate lanthanide ions, especially the Eu(III) and Tb(III) ions. The most common ligands include anionic ones such as β-diketonates[7] and aromatic carboxyl derivatives[8] and neutral ones such as phenanthridine[9] and phenyl phosphine oxide derivatives.[10] The central ions can be coordinated with identical ligands[11] or mixed ligands.[12] Among the homoleptic complexes, four bidentate or three tridentate ligands form 4:1 or 3:1 chelates with coordination numbers of 8 and 9, respectively, filling most of the first coordination sphere and thus avoiding severe quenching from coordinating water or other solvent molecules. Tridentate ligands such as pybox,[13] pyridine-2,6-dicarboxylate,[14] and bipyridine carboxylate[15] were reported to construct Eu(III) and/or Tb(III) complexes with quantum yields ranging from 20 to 85%. In general, a "hard" oxygen coordination site bonds more tightly with lanthanide (III) ion than nitrogen,[16] but the fewer choices of stable oxygen coordination sites (usually oxyacid root) limit this advantage. Meanwhile, tridentate ligands with (N^N^O) or (N^N^N) sites are not stable enough and tend to dissociate in dilute solutions. Some of them cannot even bind the lanthanide ion with all their coordinate sites as expected.[16,17] Furthermore, it is not easy to prepare a ligand that can universally and efficiently sensitize Eu(III), Tb(III), Dy(III), and Sm(III) or even more lanthanide ions because of their different energy levels and varied reduction potentials.[2a,18]

In our previous communication,[19] we integrated a hydrophobic oxygen-containing functional group diphenylphosphoryl (DPPO) to four bidentate ligands and constructed a series of tridentate ligands. Their europium(III) complexes show excellent luminescent properties with photoluminescent quantum yields (PLQYs) all over 80%. Among these, 6-

Received: February 13, 2020

Scheme 1. Synthesis Routes of the Ligand and Complexes

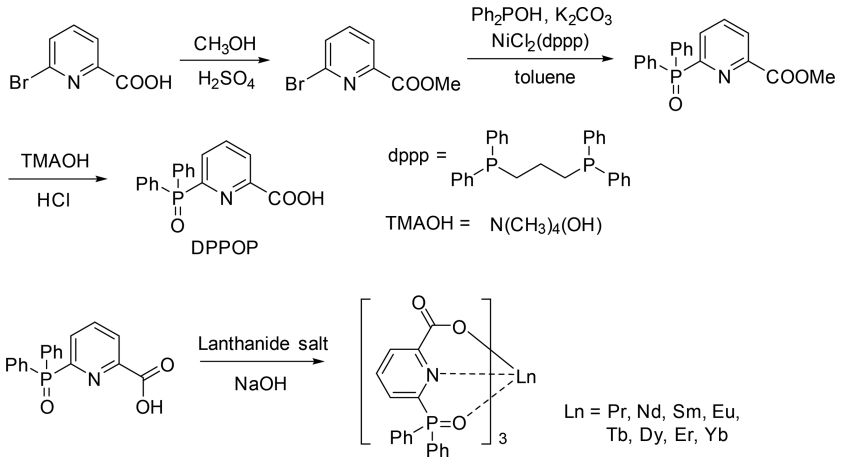

(diphenylphosphoryl)picolinate (DPPOP), which contains a carboxylate O site, a pyridine N site, and a sterically crowded diphenylphosphoryl oxygen site, possesses the highest triplet energy level of 27 780 cm^{-1} and shows the potential to sensitize a series of lanthanide ions. In this work, Pr(III), Nd(III), Sm(III), Tb(III), Dy(III), Er(III), and Yb(III) complexes employing DPPOP were prepared, yielding neutral molecules with relatively large coordination spheres. On the basis of the photophysical properties of the complexes, the energy transfer mechanism from DPPOP to the higher energy levels of lanthanide ions is proposed and verified.

RESULTS AND DISCUSSION

Synthesis and Structures. The ligand was synthesized by a previously used modified nickel-catalyzed C−P cross-coupling method[20] (Scheme 1). As the ligand is anionic and tridentate, the complexes were prepared in the stoichiometric ratio of 3:1 between the ligands and the lanthanide salts ($LnCl_3·6H_2O$ for Pr, Nd, Sm, Eu, Tb, Dy, and Er and $Ln(CF_3SO_3)_3$ for Yb). The products were obtained as crystals from methanol solutions and identified by ESI-MS, elemental analysis, and X-ray crystallography.

The single-crystal structure of Tb(III) complex is shown in Figure 1. Similar coordination environment can be observed for Pr(III), Nd(III), Sm(III), Eu(III), Dy(III), Er(III), and Yb(III) complexes (Figure S1). The central ions are coordinated by three tridentate (O^N^O) ligands with a coordination number of nine. The coordination polyhedron is categorized as distorted tricapped trigonal prism by calculating the degree of distortion of the title complexes from all possible nine-atom polyhedral structures[21] using the continuous shape measures method (Table S3).[22] In the tricapped trigonal prism, three carboxyl oxygen atoms and three phosphoryl oxygen atoms form the parallel triangle faces, and the N atoms are in the capping positions (Figure S1). The carboxyl groups and the pyridine segment are found to be nearly in the same plane (dihedral angle listed in Table 1), forming a rigid conjugated structure. Though phosphoryl groups are also located in the plane of pyridine, the sp^3 hybrid nature of phosphoryl groups makes the phenyl groups unconjugated. In the crystal structure of the Pr(III) complex, the bond lengths of Pr−O (carboxyl), Pr−N, and Pr−O (phosphoryl) are 2.4483(16), 2.6899(19), and 2.4668(16) Å, respectively. Gradually shortened bond lengths are observed for Nd-$(DPPOP)_3$, Sm$(DPPOP)_3$, Eu$(DPPOP)_3$, Tb$(DPPOP)_3$, Dy-$(DPPOP)_3$, Er$(DPPOP)_3$, and Yb$(DPPOP)_3$ (Table 1), which is due to the reduced radii of lanthanide ions known as "lanthanide contraction". This also leads to a gradually reduced degree of distortion in the tricapped trigonal prism (see the continuous shape measures values (CShM) in Table S3). The Ln−Ln distances are larger than 10.0 Å, which avoids

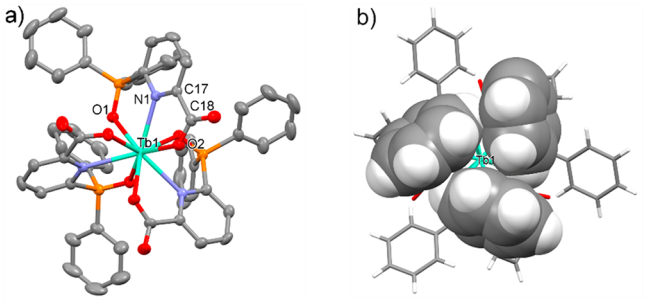

Figure 1. (a) Perspective view of Tb$(DPPOP)_3$ at the 50% probability level. Hydrogen atoms are omitted for clarity. (b) Intramolecular interaction of the edge to face C−H/π contact represented in spacefill mode of Tb$(DPPOP)_3$, with the distance between the hydrogen atom and the centroid of phenyl group being 2.774 Å. Element colors: C, gray; H, white; Tb, green; N, blue; O, red; P, orange.

Table 1. Selected Bond Lengths and Dihedral Angles of the Lanthanide Complexes

	bond lengths (Å)			
$Ln(DPPOP)_3$	Ln−O (C−O)	Ln−N	Ln−O (P═O)	dihedral angles (deg)[a]
Pr	2.4483(16)	2.6899(19)	2.4668(16)	13.37
Nd	2.432(2)	2.671(2)	2.453(2)	12.04
Sm	2.404(2)	2.642(2)	2.4273(19)	11.40
Eu	2.388(3)	2.631(4)	2.416(3)	9.48
Tb	2.366(2)	2.597(3)	2.395(2)	10.18
Dy	2.362(3)	2.601(4)	2.390(3)	10.89
Er	2.3343(19)	2.570(2)	2.3622(19)	7.94
Yb	2.3154(10)	2.5480(12)	2.3443(10)	8.57

[a]Dihedral angles of coordinating carboxyl and pyridine ring (O2−C18−C17−N1 for all complexes except for Eu complex with different labels of O11−C10−C7−N2).

https://dx.doi.org/10.1021/acs.inorgchem.0c00444
Inorg. Chem. XXXX, XXX, XXX−XXX

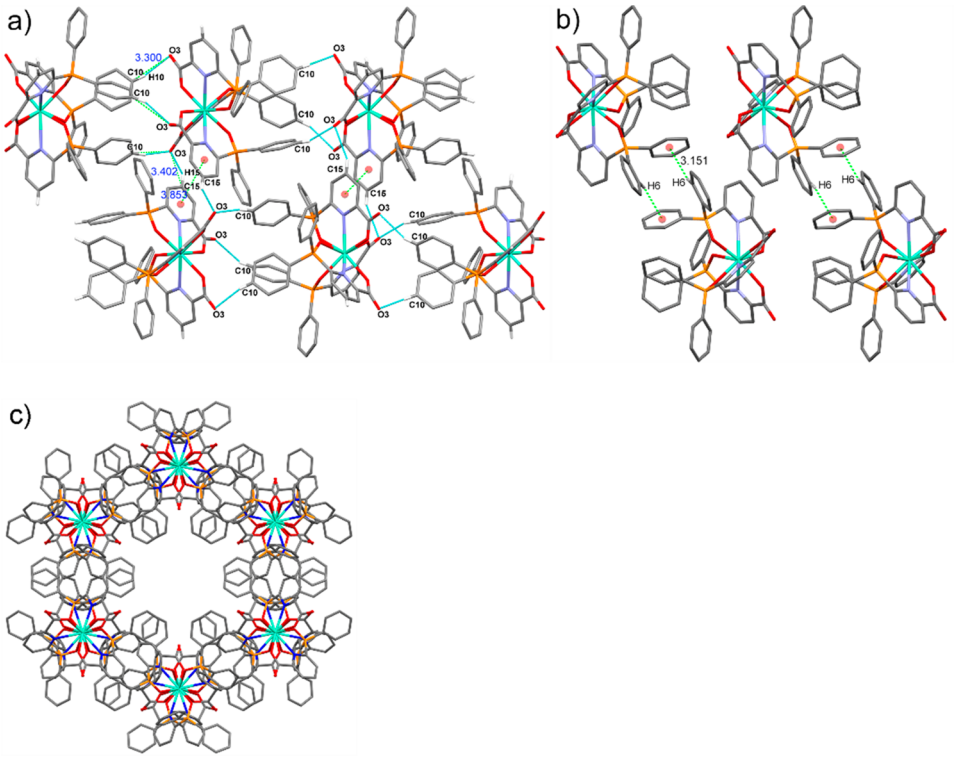

Figure 2. Intermolecular interaction of the $Tb(DPPOP)_3$ crystal (from the perpendicular view of *c*-axis): (a) Hydrogen bonds (C10−H10···O3, 3.300 Å, 158.61°; C15−H15···O3, 3.402 Å, 151.34°) and face to face $\pi-\pi$ interaction between pyridines (centroid to centroid distance of 3.853 Å). (b) Edge to face C−H/π contact with the distance between H6 and centroid of the phenyl group being 3.151 Å. (c) Packing structures of $Tb(DPPOP)_3$ viewed along the *c*-direction, showing a 1D channel along the *c*-axis filled by solvent molecules (solvent molecules are "squeezed" out). Element colors: C, gray; Tb, green; N, blue; O, red; P, orange. Hydrogen atoms are omitted for clarity except those for intermolecular interactions in (a) and (b).

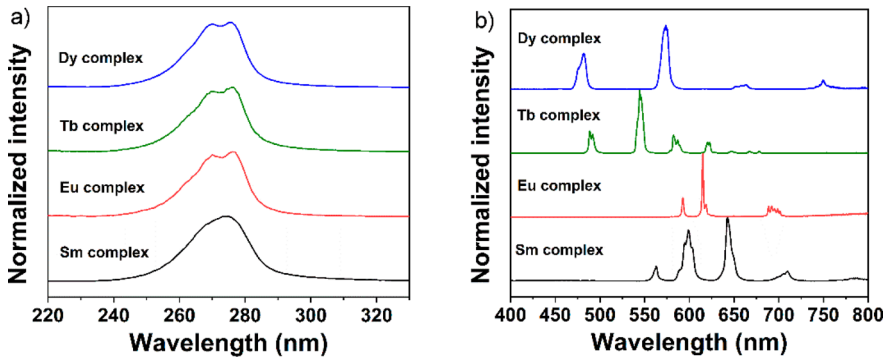

Figure 3. (a) Excitation spectra of Sm(III), Eu(III), Tb(III), and Dy(III) complexes in CH_2Cl_2 solutions (1×10^{-5} M, λ_{em} = 644, 615, 545, and 572 nm, respectively). (b) Emission spectra of the title complexes in the solid state (λ_{ex} = 280 nm).

concentration quenching and is favorable for efficient luminescence.

The complexes exhibit C_3-symmetry with three ligands arranged in the same direction ("up−up−up"), which is uncommon.[23] Specifically, the sterically crowded diphenylphosphoryl groups are located in the same side. It is found that strong intramolecular C−H/π contacts (edge-to-face)[24] exist between the diphenylphosphoryl groups with distances of 2.75−2.80 Å (Figures 1b and S2−S9), which is responsible for the stabilization of such a sterically crowded configuration. Intermolecular interactions (taking the terbium(III) complex for example) may also contribute to the stabilization of the special packing mode. These interactions include the hydrogen bonds between the carboxyl oxygen and the phenyl C−H (C10−H10···O3, 3.300 Å, 158.61°; C15−H15···O3, 3.402 Å, 151.34°, Figure 2a), the face-to-face $\pi-\pi$ interaction of the pyridine rings (centroid to centroid distance of 3.853 Å, Figure 2a), and the C−H/π contact of diphenylphosphoryl groups from different complex molecules (with the distance between H6 and the centroid of the phenyl group being 3.151 Å, Figure 2b). Similar intermolecular interactions for other complexes can be found in Figures S10−S16. More interestingly, 1D channels along the *c*-axis are observed in the crystal structure of these complexes with accessible radii of ∼5.0 Å (considering the van der Waals radius of atoms), and these channels are filled by solvent molecules (Figures 2c and S17, solvent molecules are "squeezed" out).[25]

https://dx.doi.org/10.1021/acs.inorgchem.0c00444
Inorg. Chem. XXXX, XXX, XXX−XXX

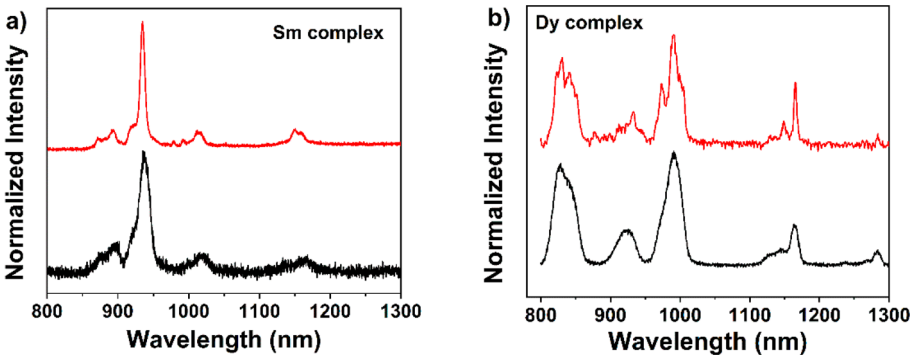

Figure 4. NIR emission spectra of the Sm(III) (a) and Dy(III) complexes (b) in crystals (red) and 1×10^{-5} M CH_2Cl_2 solutions (black). λ_{ex} is 275 nm for solutions and 280 nm for solids.

Luminescence of Sm(III), Eu(III), Tb(III), and Dy(III) Complexes. These complexes are highly luminescent both in the solid state and in solutions when excited by short-wavelength UV light. The excitation profiles of the four complexes in CH_2Cl_2 solutions are identical, which correspond to the ligand absorption (Figures 3a and S18). As discussed in our previous communication, the introduction of the diphenylphosphoryl (sp^3 hybrid) does not greatly change the energy level of picolinate, so the absorption and excitation data of the DPPOP complex are similar to those of the picolinate-based complexes.[19] The high energy excitation is advantageous in certain applications such as anticounterfeiting inks (254 nm excitable and 365 nm not excitable). The characteristic line emission spectra of the lanthanide complexes in the visible range are shown in Figure 3b.

Among the complexes studied here, the Eu(III) and Tb(III) complexes give emissions only in the visible region. For $Eu(DPPOP)_3$, the five distinct peaks at 580, 592, 615, 650, and 692 nm correspond to the transitions of $^5D_0$ to ^7F_J (J = 0–4), with the electric-dipole transition band at 615 nm being the strongest. In the range of 500–570 nm, three weak emissions at 526, 537, and 558 nm can also be observed (Figure S19), which originate from the transitions of $^5D_1$ to ^7F_J (J = 0–2).[26] The emission spectrum of the Tb(III) complex shows characteristic peaks at 489, 544, 582, 620, 647, 668, and 678 nm, which are assigned to the transitions of $^5D_4$ to ^7F_J (J = 6–0), with the emission at 544 nm being the strongest.

The Sm(III) and Dy(III) complexes emit light in both the visible and near-infrared (NIR) regions. For $Sm(DPPOP)_3$, the visible emission peaks at 563, 599, 643, 710, and 785 nm corresponds to $^4G_{5/2} \rightarrow {}^6H_J$ (J = 5/2–13/2) transitions, and that located at 532 nm corresponds to the higher energy level transition of $^4F_{3/2} \rightarrow {}^6H_{5/2}$ (Figures 3b and S19). In addition to the visible emission, $Sm(DPPOP)_3$ gives intense NIR emissions at 870, 893, 935, 1014, and 1151 nm, corresponding to $^4G_{5/2} \rightarrow {}^6F_J$, ($J$ = 1/2–9/2, Figure 4a). For $Dy(DPPOP)_3$, four strong peaks at 480, 574, 662, and 750 nm corresponding to $^4F_{9/2} \rightarrow {}^6H_J$ (J = 15/2–9/2) and one weak peak at 455 nm corresponding to $^4I_{15/2} \rightarrow {}^6H_{15/2}$ are observed (Figures 3b and S19). Notably, the Dy(III) complex emits a warm-white light with a CIE coordinate of (0.36, 0.42) and a color temperature of about 4500 K. The NIR emissions of $Dy(DPPOP)_3$ are also measured and shown in Figure 4b. We observe distinct emission peaks at 826, 923, 990, 1164, and 1283 nm, which correspond to the transitions of $^4F_{9/2} \rightarrow {}^6H_{7/2}$ (or $^6F_{9/2}$), $^6H_{5/2}$, $^6F_{7/2}$, $^6F_{5/2}$, and $^6F_{11/2}$ (or $^6H_{9/2}$) $\rightarrow {}^6H_{15/2}$, respectively.[27]

It is known that the details in the emission spectra of one lanthanide complex, including precise emission wavelength, relative intensity, and peak splitting, are largely related to the coordinating environment of the central ion. Taking $Eu(DPPOP)_3$ for example, the crystal field splitting leads to 1, 1, 3, and at least 5 components for $^5D_0$ to ^7F_J transitions (J = 0, 1, 2, and 4) in the solid state (Figure S20). This is almost consistent with the peak splitting predictions for the Eu(III) complex having a C_3 symmetry with 1, 2, 3, and 6 components for the above transitions.[26a,28] By comparing the emission spectra of $Eu(DPPOP)_3$ in crystals, in CH_2Cl_2 solutions, and in a coordinating dimethylsulfoxide (DMSO)/water (v/v = 1:1) solution, we can see similar splitting conditions (only broadened peaks are shown in solution due to solvation) and an unchanged proportion of emission intensity at different wavelengths (Figure S20), which indicates that the coordination environment in crystals and solutions are nearly identical. This shows the good coordination stability of the complex without much dissociation in solutions. A similar situation can be observed for Sm(III), Tb(III), and Dy(III) complexes (Figure S20).

The luminescence decay curves of the title complexes were measured (Figures 5 and S21–S23). All of these are fitted as a single exponential with lifetime values (τ_{obs}) shown in Table 2. Long lifetimes of 2.8 (2.5) and 2.4 (2.4) ms in CH_2Cl_2 (or DMSO/water) solutions are obtained for $Eu(DPPOP)_3$ and $Tb(DPPOP)_3$, respectively, indicating that the parity-forbid-

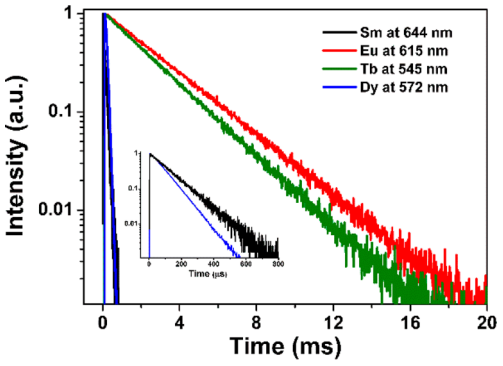

Figure 5. Emission intensity decay curves of $Sm(DPPOP)_3$ (black), $Eu(DPPOP)_3$ (red), $Tb(DPPOP)_3$ (green), and $Dy(DPPOP)_3$ (blue) in CH_2Cl_2 solutions monitored at 644, 615, 545, and 572 nm, respectively. Inset: decay curves for $Sm(DPPOP)_3$ and $Dy(DPPOP)_3$ in a shorter time range. Conditions: concentration = 1×10^{-5} M, λ_{ex} = 275 nm.

https://dx.doi.org/10.1021/acs.inorgchem.0c00444
Inorg. Chem. XXXX, XXX, XXX–XXX

Table 2. Lifetimes and Quantum Yields of Ln(DPPOP)$_3$

	solid		solution	
Ln(DPPOP)$_3$	τ_{obs}(ms)	Φ_L^{Ln} (%)	τ_{obs}(ms)	Φ_L^{Ln} (%)[c]
Sm	0.089	4.2 ± 0.6	0.11,[b] 0.060[c]	n.a.
Eu	2.4	80.8 ± 1.1	2.8,[b] 2.5[c]	53.4 ± 0.3
Tb	1.9	97.4 ± 3.5	2.4,[b] 2.4[c]	52.3 ± 0.5
Dy	0.067	13.1 ± 0.1, 15.5 ± 0.1[a]	0.080,[b] 0.050[c]	3.7 ± 0.3
Nd	1.2×10^{-3}	n.a.	n.a.	n.a.
Er	2.1×10^{-3}	n.a.	n.a.	n.a.
Yb	0.019	n.a.	n.a.	n.a.

[a]Absolute quantum yields measured upon desolvation. [b]Lifetime measured in 1×10^{-5} M CH_2Cl_2 solutions. [c]Lifetime and absolute quantum yields measured in 1×10^{-4} M DMSO/water (v/v = 1:1) solutions. n.a. = Not available due to weak emission intensities.

den f–f transitions are barely quenched by the environment. A reduced lifetime for the Eu(III) complex in the solid state is observed due to the refractive index of the solid (usually considered as 1.5) being higher than that in solvents (1.42 for CH_2Cl_2 and 1.41 for 1:1 DMSO/water). The lifetimes of Sm(DPPOP)$_3$ and Dy(DPPOP)$_3$ are much shorter (110 and 80 μs in CH_2Cl_2 solutions, respectively) compared with those of Eu(DPPOP)$_3$ and Tb(DPPOP)$_3$. This is rational considering that the NIR emissions of Sm(III) and Dy(III) complexes are more easily quenched by the small energy oscillators such as C–H and C=O.[29] In DMSO/water solutions, the lifetimes reduced to 60 and 50 μs for Sm(DPPOP)$_3$ and Dy(DPPOP)$_3$, respectively, which suffer from severe quenching by water molecules.

We measured the absolute quantum yields (Φ_L^{Ln}) for the complexes in both crystals and DMSO/water (v/v = 1:1) solutions by using an integral sphere and the results are shown in Table 2. The crystals of Eu(DPPOP)$_3$ and Tb(DPPOP)$_3$ showed remarkable quantum yields as high as 81 and 97%, respectively, indicating the very high efficiency of energy transfer and barely any energy quenching pathways. This benefits from the compact, stable, and saturated coordination in the DPPOP-based complexes. In DMSO/water (v/v = 1:1) solutions, high quantum yields of over 50% can still be observed for Eu(III) and Tb(III) complexes. The radiative rate constant (k_r) was calculated to be 269 s^{-1} according to eqs 2 and 3 for Eu(III) complex, similar to those of the complexes based on 8-hydroxy-1,5-naphthyridine-2-carboxylic acid (200–300 s^{-1}, crystallized in $R\bar{3}$ space group with C_3-symmetry)[23b] but not as high as those of the complexes based on bidentate 8-hydroxy-1,5-naphthyridine (500–700 s^{-1})[30] and β-diketonates (over 500 s^{-1}),[31] which crystallize in the orthorhombic, monoclinic, or triclinic crystal systems. The symmetry of the coordination environment may account for the difference in k_r.[23a] The hypersensitive electric-dipole transition of $^5D_0 \rightarrow {}^7F_2$ is in close relation to the coordination environment: The higher the coordination symmetry, the lower the hypersensitive transition, and thus the lower the E_{TOT}/E_{MD} value (ratio between the integrated emission spectrum and the integrated emission band of the magnetic dipole transition from $^5D_0$ to $^7F_1$, E_{MD} being independent of the coordination environment). From eq 2, we can see that k_r is proportional to E_{TOT}/E_{MD}, suggesting that a high coordination symmetry leads to low k_r. Although the radiative rate constant is low, the central Eu^{III} ion is shielded well by ligands, resulting in a low nonradiative rate constant (k_{nr}) of 128 s^{-1} and consequently a high intrinsic quantum yield of 68% (eq 4, Table S4).

The quantum yields of Dy(DPPOP)$_3$ in the visible range (4% in DMSO/water solution and 13% in the crystal state) are lower than those of Eu(DPPOP)$_3$ and Tb(DPPOP)$_3$. This is due to the easier quenching of its emissive excited states (giving NIR emission) by the small energy oscillators such as the C–H vibration. The quantum yield is comparable with the results reported for Dy(III) complexes, even for those based on fully fluorinated ligands.[32] The much lower quantum yield of Sm(DPPOP)$_3$ in the visible range (4% in the solid state) is also among the sizable values for samarium(III) complexes emitting in both the visible and NIR regions.[10,33]

Energy Transfer Mechanism. In the luminescent process of a lanthanide complex, the most common energy transfer pathways involve[34] (1) light absorption by ligands resulting in singlet excited states; (2) intersystem crossing (ISC) from the singlet to triplet excited states; (3) energy transfer from the ligand to the lanthanide ion; and (4) deactivation via the radiation of the lanthanide ion (Figure 6). In many cases, the rate of the ISC is much larger than that of the energy transfer from singlet state to lanthanide ion,[35] so the sensitization process takes place through triplet states of the organic ligand.[36] In other cases, the sensitization is either mostly or partially singlet mediated.[37] The energy transfer efficiency relies on the energy difference between the donating and accepting energy levels, both for the Förster and Dexter transfer mechanism.[38]

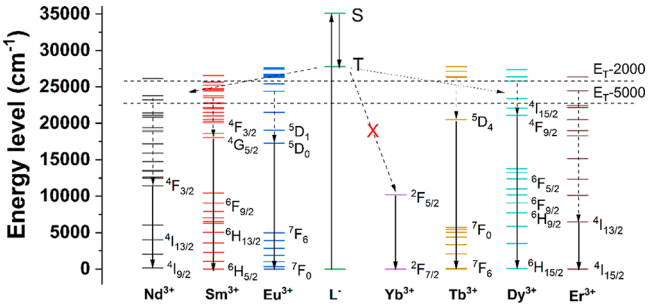

Figure 6. Proposed mechanism for the ligand–Ln(III) energy transfer (simplified Ln(III) energy levels are obtained from literatures[39]). S and T stand for the lowest singlet and triplet excited states of the ligand in solutions, respectively. The dashed horizontal lines show energy levels below 2000 and 5000 cm^{-1} of the lowest triplet energy level (E_T).

In general, the energy level of the donor should be higher than that of the acceptor (i.e., the lanthanide ion) to realize successful sensitization (usually in the range of 2000–5000 cm^{-1}).[2a,40] An insufficient energy difference may lead to back energy transfer, while an excessively large one results in poor energy transfer efficiency. For the complexes studied in this work, the energy transfer takes place most probably through the triplet states. However, the energy differences between the lowest triplet state E_T (27 780 cm^{-1}, Figure S24) and the emitting levels of these lanthanide ions (18 100, 17 200, 20 400, and 21 100 cm^{-1} for Sm^{III}, Eu^{III}, Tb^{III}, and Dy^{III} ions, respectively, Figure 6) seem to be too large (6680–10 580 cm^{-1}) for efficient energy transfer, which seems to contradict the excellent quantum yields and high sensitization efficiencies of the Eu(III) and Tb(III) complexes. Therefore, it is plausible to propose that sensitization of these lanthanide ions takes

https://dx.doi.org/10.1021/acs.inorgchem.0c00444
Inorg. Chem. XXXX, XXX, XXX–XXX

place most possibly through higher excited states of lanthanide ions, which serve as intermediate levels and undergoes fast internal conversion to the low lying emitting levels. Weak emissions from the second excited states ($^5D_1$ for Eu^{III}, $^4F_{3/2}$ for Sm^{III}, and $^4I_{15/2}$ for Dy^{III} ion) can be observed in Figure S19, which proves that the energy transfer undergoes these second excited state. As the rate of internal conversion is always several magnitudes larger than that of the parity-forbidden lanthanide emission,[26b] it is expected that no emission peaks from transitions of higher excited states or only very weak emissions from the second excited states can be observed.

When no intermediate levels exist in lanthanide complex with a large donor−acceptor energy level difference, one can expect inefficient energy transfer, which is the case with our NIR-emitting Yb(III) complex (the Yb^{III} ion has only one accepting energy level of 10 200 cm^{-1}). Usually, Yb(III) complexes show a stronger NIR emission intensity at 980 nm compared to that of its Nd(III)- and Er(III)-based counterparts whose emissions lie at even longer wavelengths and endure more severe quenching by C−H and O−H vibrations.[41] However, in our system, a faint emission around 980 nm for the Yb(III) complex was detected in crystals (intensity similar to that of the Er(III) complex at 1515 nm), while the Nd(III) complexes showed much stronger NIR emissions (Figure 7). The high energy transfer efficiency of the

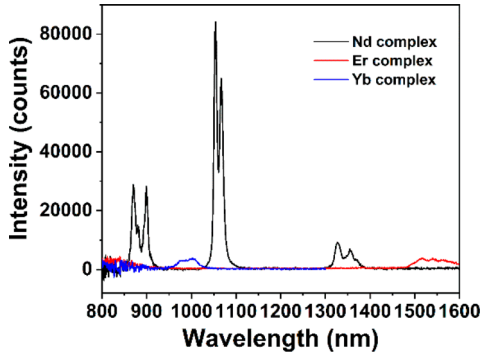

Figure 7. Emission spectra of $Nd(DPPOP)_3$, $Er(DPPOP)_3$, and $Yb(DPPOP)_3$ complexes in crystals. λ_{ex} = 290 nm for Nd(III) and Yb(III) complexes and 300 nm for Er(III) complex.

Eu(III) complex (78% in DMSO/water solution, Table S4) shows that quenching pathways such as low energy LMCT state or photoinduced electron transfer process barely exists, which means the energy level of $DPPOP^+−Eu^{2+}$ is higher than the $^5D_0$ level of the Eu^{III} ion. As the standard reduction potential of Yb^{III}/Yb^{II} is lower than that of Eu^{III}/Eu^{II}, the energy level of $DPPOP^+−Yb^{2+}$ must be higher than that of $DPPOP^+−Eu^{2+}$ (over 17 200 cm^{-1}), so there exists no such quenching pathway for the title Yb(III) complex. As proposed by Horrocks et al., the $ligand^+−Yb^{2+}$ state may serve as the intermediate state for the energy transfer in Yb(III) complex with large donor−acceptor energy difference.[6a] However, in this work, the energy difference between $DPPOP^+−Yb^{2+}$ and $^2F_{5/2}$ (10 200 cm^{-1}) is still very large (at least over 7000 cm^{-1}, the exact value not investigated here), which may account for the faint emission of the Yb(III) complex. By comparing the emission intensities of Yb(III) and Nd(III) complex with identical DPPOP ligands, one can ascribe the weak emission of Yb(III) complex to the inefficient energy transfer caused by the large energy difference between the donor (ligand's triplet state or photoinduced electron transfer state) and the $^2F_{5/2}$ level of the Yb^{III} ion.

Quantum Yield Change upon Dehydration and Rehydration of Dy(III) Complex. As discussed in the "Synthesis and Structures" section, the 1D channels along the *c*-axis of the crystals are filled by solvent molecules. TGA curves of Sm(III), Eu(III), Tb(III), and Dy(III) complexes under nitrogen flow were recorded and shown in Figure S25. We can see a weight loss of 5−15% below 90 °C, which corresponds to the complete loss of solvent molecules in the crystals. The complexes are then stable before decomposing at 390 °C. We tested the absolute quantum yield of $Dy(DPPOP)_3$ upon heating (120 °C), which increases to 16% from an original value of 13% benefiting from the elimination of the vibration quenching from the solvent in the channels. We then alternately dehydrated (120 °C for 5 h) and rehydrated (water vapor saturated overnight) the sample of $Dy(DPPOP)_3$ in three cycles, and found that the quantum yield changes reversibly (Figure 8). This suggests that the complex may find application as sensitive luminescent sensors for certain vapors such as moisture.

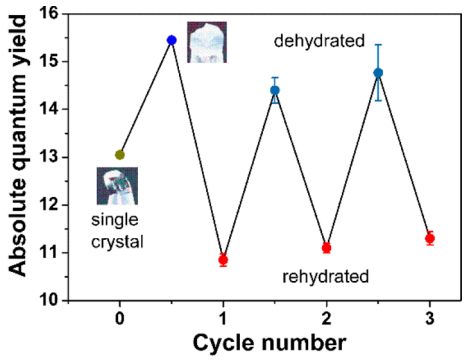

Figure 8. Absolute quantum yield of $Dy(DPPOP)_3$ upon dehydration and rehydration, showing reversible luminescence change. Insets are the photographs of the as-prepared single crystal and the dehydrated one.

CONCLUSIONS

To summarize, we have synthesized a series of highly emissive lanthanide complexes by using an (O^N^O) tridentate ligand DPPOP. The ligand perfectly protects the central lanthanide ion from the exterior quenching environment when forming 3:1 complexes. Due to the high energy transfer efficiency and suppressed nonradiative deactivation, brilliant overall quantum yields of 81, 97, 13, and 4% and long lifetimes of 2.4, 1.9, 0.067, and 0.089 ms were obtained in the solid state for Eu(III), Tb(III), Dy(III), and Sm(III) complexes, respectively. While strong NIR-emissions of the Nd(III) complex were observed, the Yb(III) complex only showed faint NIR emission, which is ascribed to the large energy difference between DPPOP and the Yb^{III} ion. The 1D channels in crystals enable the Dy(III) complex to absorb and eliminate water reversibly, leading to a reversible quantum yield change.

EXPERIMENTAL SECTION

General Information. Electrospray ionization mass spectra (ESI-MS) were performed in positive or negative ion mode on Bruker Apex IV Fourier transform ion cyclotron resonance mass spectrometer.

https://dx.doi.org/10.1021/acs.inorgchem.0c00444
Inorg. Chem. XXXX, XXX, XXX−XXX

Elemental analyses were measured on a VARIO elemental analyzer from Elementar Analysensysteme GmbH. UV−visible absorption spectra were measured by a PerkinElmer Lambda 35 spectrometer. Emission and low-temperature phosphorescence spectra were recorded on the Edinburgh FLS920/980 fluorescence spectrophotometer. Luminescence lifetimes were obtained on a single photon counting spectrometer from Edinburgh FLS920/980 with a microsecond pulse lamp or variable pulsed diode laser (375 and 450 nm) as the excitation source. The data were analyzed by the tail fit of the decay profile using a software package provided by Edinburgh Instruments. Thermal gravimetric analysis (TGA) was carried out on Q600SDT instruments at an elevation temperature rate of 10 °C min^{-1} under 100 mL min^{-1} nitrogen flow.

The photophysical properties of the complexes were carried out in CH_2Cl_2 or DMSO/water (v/v = 1:1) solutions and in the solid states. For routine measurements, the complexes were dissolved in a CH_2Cl_2 and methanol (v/v = 10:1) or DMSO solution with an initial concentration of 1×10^{-3} M and diluted to the concentration needed by CH_2Cl_2 or DMSO/water solution. All measurements were performed at room temperature except the phosphorescence experiments at 77 K.

Synthesis of the Lanthanide Complexes. Synthesis of the ligand can be seen in ref 19.

Sm(DPPOP)$_3$. To the methanol solution of deprotonated ligand was added $SmCl_3 \cdot 6H_2O$ in the molar ratio of 3:1. After reflux for 0.5 h, the solution was cooled to room temperature, and crystals grew through volatilization of solvent. Colorless crystals were obtained and filtered with care. ESI-MS positive: Calcd 1118.1, m/z = 1119.1 (M + H^+). Anal. Calcd for $C_{54}H_{39}SmN_3O_9P_3 \cdot 2H_2O$: C, 56.24, H, 3.76, N, 3.64. Found: C, 56.08, H, 3.51, N, 4.09%.

All the other complexes Ln(DPPOP)$_3$ (Ln = Pr, Nd, Eu, Tb, Dy, Er, and Yb) were synthesized in a manner similar to that used for Sm(DPPOP)$_3$, except Yb(III) complex which used Yb$(CF_3SO_3)_3$ as lanthanide salt.

Pr(DPPOP)$_3$. Green crystals. ESI-MS positive: Calcd 1107.1, m/z = 1108.1 (M + H^+), 1130.1 (M+Na^+). Anal. Calcd for $C_{54}H_{39}PrN_3O_9P_3 \cdot H_2O$: C, 57.65, H, 3.67, N, 3.74. Found: C, 57.52, H, 3.74, N, 3.74%.

Nd(DPPOP)$_3$. Purple crystals. ESI-MS positive: Calcd 1110.1, m/z = 1133.1 (M+Na^+). Anal. Calcd for $C_{54}H_{39}NdN_3O_9P_3 \cdot 1.5H_2O$: C, 56.99, H, 3.72, N, 3.69. Found: C, 56.85, H, 3.63, N, 3.67%.

Eu(DPPOP)$_3$. Colorless crystals. ESI-MS positive: Calcd 1119.1, m/z = 1120.1 (M + H^+). Anal. Calcd for $C_{54}H_{39}EuN_3O_9P_3 \cdot H_2O$: C, 57.05, H, 3.64, N, 3.70. Found: C, 57.21, H, 3.70, N, 3.70%.

Tb(DPPOP)$_3$. Colorless crystals. ESI-MS positive: Calcd 1125.1, m/z = 1126.1 (M + H^+), 1148.1 (M+Na^+). Anal. Calcd for $C_{54}H_{39}TbN_3O_9P_3 \cdot H_2O$: C, 56.71, H, 3.61, N, 3.67. Found: C, 56.74, H, 3.66, N, 3.66%.

Dy(DPPOP)$_3$. Colorless crystals. ESI-MS positive: Calcd 1130.1, m/z = 1131.1 (M + H^+). Anal. Calcd for $C_{54}H_{39}DyN_3O_9P_3 \cdot 2H_2O$: C, 55.66, H, 3.72, N, 3.61. Found: C, 55.34, H, 3.93, N, 3.52%.

Er(DPPOP)$_3$. Pink crystals. ESI-MS positive: Calcd 1132.1, m/z = 1155.1 (M + Na^+). Anal. Calcd for $C_{54}H_{39}ErN_3O_9P_3 \cdot 0.5H_2O$: C, 56.74, H, 3.53, N, 3.68. Found: C, 56.90, H, 3.46, N, 3.70%.

Yb(DPPOP)$_3$. Colorless crystals. ESI-MS positive: Calcd 1140.1, m/z = 1141.1 (M + H^+), 1163.1 (M+Na^+). Anal. Calcd for $C_{54}H_{39}YbN_3O_9P_3 \cdot 3.5H_2O$: C, 53.92, H, 3.85, N, 3.49. Found: C, 53.93, H, 3.81, N, 3.42%.

X-ray Crystallographic Study. The single crystal of the corresponding complexes was obtained by slow crystallization of their methanol solution. The structures were determined from single-crystal X-ray diffraction data (collected at Rigaku RAPID-S image plate diffractometer or Rigaku single-crystal X-ray diffractometer) and refined with SHELXL-2014/2015 program package. Solvent molecules are "squeezed" out.[25] The volumes that were "squeezed" out within the bounds of the unit cell amount to 1365, 1387, 1376, 1349, 1326, 1392, and 1440 Å^3 for Pr(III), Nd(III), Sm(III), Tb(III), Dy(III), Er(III), and Yb(III) complex, respectively. The electron counts in these voids are 380, 371, 399, 366, 257, 378, and 304, respectively.

Quantum Yield Measurements and Luminescence Parameters. Absolute overall quantum yields (Φ_L^{Ln}) were measured by the C9920−02 absolute quantum yield measurement system from Hamamatsu Company using an integral sphere. The energy transfer efficiency (η_{sens}) and intrinsic quantum yield (Φ_{Eu}^{Eu}) of Eu(III) complex are calculated from eq 1 as follows.[42]

$$\Phi_L^{Eu} = \eta_{sens} \times \Phi_{Eu}^{Eu} = \eta_{sens} \times \frac{\tau_{obs}}{\tau_R} \quad (1)$$

τ_{obs} is the emission lifetime determined by experiment and τ_R is the radiative lifetime. For Eu(III) ion, τ_R can be obtained by eq 2:

$$\frac{1}{\tau_R} = A_{MD} n^3 (E_{TOT}/E_{MD}) \quad (2)$$

where E_{TOT}/E_{MD} is the ratio of integrated emission spectrum and integrated emission band of a magnetic dipole transition ($^5D_0$ to $^7F_1$ for Eu^{3+}). A_{MD} is the spontaneous emission probability of the $^5D_0$ to $^7F_1$ transition being 14.65 s^{-1}, and n is the refractive index of the solution.

$$k_r = 1/\tau_R \quad (3)$$

$$k_{nr} = 1/\tau_{obs} - k_r \quad (4)$$

■ ASSOCIATED CONTENT

Supporting Information

The Supporting Information is available free of charge at https://pubs.acs.org/doi/10.1021/acs.inorgchem.0c00444.

Crystal structures and crystallographic data; luminescence decay curves in the solid state; emission spectra in solution; TGA curves (PDF)

Accession Codes

CCDC 1508078, 1508099, 1508107, 1981494, and 1981496−1981498 contain the supplementary crystallographic data for this paper. These data can be obtained free of charge via www.ccdc.cam.ac.uk/data_request/cif, or by emailing data_request@ccdc.cam.ac.uk, or by contacting The Cambridge Crystallographic Data Centre, 12 Union Road, Cambridge CB2 1EZ, UK; fax: +44 1223 336033.

■ AUTHOR INFORMATION

Corresponding Authors

Huibo Wei − *Jiangsu JITRI Molecular Engineering Institute Co., Ltd., Changshu 215500, China*; Email: weihuibo@163.com

Zuqiang Bian − *Beijing National Laboratory for Molecular Sciences, State Key Laboratory of Rare Earth Materials Chemistry and Applications, College of Chemistry and Molecular Engineering, Peking University, Beijing 100871, China*; orcid.org/0000-0003-1554-6279; Email: bianzq@pku.edu.cn

Authors

Chen Wei − *Beijing National Laboratory for Molecular Sciences, State Key Laboratory of Rare Earth Materials Chemistry and Applications, College of Chemistry and Molecular Engineering, Peking University, Beijing 100871, China*; orcid.org/0000-0002-8065-1991

Boxun Sun − *Beijing National Laboratory for Molecular Sciences, State Key Laboratory of Rare Earth Materials Chemistry and Applications, College of Chemistry and Molecular Engineering, Peking University, Beijing 100871, China*

Zifeng Zhao − *Beijing National Laboratory for Molecular Sciences, State Key Laboratory of Rare Earth Materials*

https://dx.doi.org/10.1021/acs.inorgchem.0c00444
Inorg. Chem. XXXX, XXX, XXX−XXX

Chemistry and Applications, College of Chemistry and Molecular Engineering, Peking University, Beijing 100871, China; orcid.org/0000-0002-5182-059X

Zelun Cai − *Beijing National Laboratory for Molecular Sciences, State Key Laboratory of Rare Earth Materials Chemistry and Applications, College of Chemistry and Molecular Engineering, Peking University, Beijing 100871, China*

Jiajia Liu − *Beijing National Laboratory for Molecular Sciences, State Key Laboratory of Rare Earth Materials Chemistry and Applications, College of Chemistry and Molecular Engineering, Peking University, Beijing 100871, China*

Yu Tan − *Beijing National Laboratory for Molecular Sciences, State Key Laboratory of Rare Earth Materials Chemistry and Applications, College of Chemistry and Molecular Engineering, Peking University, Beijing 100871, China*

Zhiwei Liu − *Beijing National Laboratory for Molecular Sciences, State Key Laboratory of Rare Earth Materials Chemistry and Applications, College of Chemistry and Molecular Engineering, Peking University, Beijing 100871, China;* orcid.org/0000-0003-3001-5310

Chunhui Huang − *Beijing National Laboratory for Molecular Sciences, State Key Laboratory of Rare Earth Materials Chemistry and Applications, College of Chemistry and Molecular Engineering, Peking University, Beijing 100871, China*

Complete contact information is available at: https://pubs.acs.org/10.1021/acs.inorgchem.0c00444

Notes

The authors declare no competing financial interest.

■ ACKNOWLEDGMENTS

We thank Prof. Zheming Wang and Mr. Ziran Zhao for constructive discussion and Dr. Jie Su and Dr. Zhengyang Zhou for single-crystal XRD refinement. This research is supported through grants from the National Basic Research Program of China (Grant 2017YFA0205100), National Natural Science Foundation of China (Grant 21621061), Key Project of Science and Technology Plan of Beijing Education Commission (Grant KZ201910028038), and Natural Science Foundation of Beijing Municipality (Grant 2172017).

■ REFERENCES

(1) (a) Bünzli, J.-C. G. Lanthanide light for biology and medical diagnosis. *J. Lumin.* **2016**, *170*, 866−878. (b) Sy, M.; Nonat, A.; Hildebrandt, N.; Charbonniere, L. J. Lanthanide-based luminescence biolabelling. *Chem. Commun.* **2016**, *52*, 5080−5095.

(2) (a) Parker, D. Luminescent lanthanide sensors for pH, pO_2 and selected anions. *Coord. Chem. Rev.* **2000**, *205*, 109−130. (b) Wang, X.; Chang, H.; Xie, J.; Zhao, B.; Liu, B.; Xu, S.; Pei, W.; Ren, N.; Huang, L.; Huang, W. Recent developments in lanthanide-based luminescent probes. *Coord. Chem. Rev.* **2014**, *273*−*274*, 201−212.

(3) Wang, L.; Zhao, Z.; Wei, C.; Wei, H.; Liu, Z.; Bian, Z.; Huang, C. Review on the Electroluminescence Study of Lanthanide Complexes. *Adv. Opt. Mater.* **2019**, *7*, 1801256.

(4) Wei, C.; Ma, L.; Wei, H.; Liu, Z.; Bian, Z.; Huang, C. Advances in luminescent lanthanide complexes and applications. *Sci. China: Technol. Sci.* **2018**, *61*, 1265−1285.

(5) Crosby, G. A.; Whan, R. E.; Alire, R. M. Intramolecular Energy Transfer in Rare Earth Chelates. Role of the Triplet State. *J. Chem. Phys.* **1961**, *34*, 743−748.

(6) (a) Horrocks, W. D., Jr.; Bolender, J. P.; Smith, W. D.; Supkowski, R. M. Photosensitized Near Infrared Luminescence of Ytterbium(III) in Proteins and Complexes Occurs via an Internal Redox Process. *J. Am. Chem. Soc.* **1997**, *119*, 5972−5973. (b) Beeby, A. M.; Clarkson, I. S.; Dickins, R.; Faulkner, S.; Parker, D.; Royle, L. S.; de Sousa, A. A.; Williams, J. A. G.; Woods, M. Non-radiative deactivation of the excited states of europium, terbium and ytterbium complexes by proximate energy-matched OH, NH and CH oscillators: an improved luminescence method for establishing solution hydration states. *J. Chem. Soc., Perkin Trans. 2* **1999**, 493−504.

(7) (a) Filipescu, N.; Mushrush, G. W.; Hurt, C. R.; McAvoy, N. Fluorescence Quantum Efficiencies of Octa-coordinated Europium Homogeneous and Mixed Chelates in Organic Solvents. *Nature* **1966**, *211*, 960−961. (b) Shi, M.; Li, F.; Yi, T.; Zhang, D.; Hu, H.; Huang, C. Tuning the Triplet Energy Levels of Pyrazolone Ligands to Match the $^5D_0$ Level of Europium(III). *Inorg. Chem.* **2005**, *44*, 8929−8936.

(8) (a) Gassner, A.-L.; Duhot, C. G.; Bünzli, J.-C. G.; Chauvin, A.-S. Remarkable Tuning of the Photophysical Properties of Bifunctional Lanthanide tris(Dipicolinates) and its Consequence on the Design of Bioprobes. *Inorg. Chem.* **2008**, *47*, 7802−7812. (b) Chow, C. Y.; Eliseeva, S. V.; Trivedi, E. R.; Nguyen, T. N.; Kampf, J. W.; Petoud, S.; Pecoraro, V. L. Ga^{3+}/Ln^{3+} Metallacrowns: A Promising Family of Highly Luminescent Lanthanide Complexes That Covers Visible and Near-Infrared Domains. *J. Am. Chem. Soc.* **2016**, *138*, 5100−5109.

(9) Dasari, S.; Abbas, Z.; Kumar, P.; Patra, A. K. Photosensitized samarium(iii) and erbium(iii) complexes of planar N, N-donor heterocyclic bases: crystal structures and evaluation of biological activity. *CrystEngComm* **2016**, *18*, 4313−4322.

(10) Miyata, K.; Nakagawa, T.; Kawakami, R.; Kita, Y.; Sugimoto, K.; Nakashima, T.; Harada, T.; Kawai, T.; Hasegawa, Y. Remarkable Luminescence Properties of Lanthanide Complexes with Asymmetric Dodecahedron Structures. *Chem. - Eur. J.* **2011**, *17*, 521−528.

(11) Shavaleev, N. M.; Gumy, F.; Scopelliti, R.; Bünzli, J.-C. G. Highly Luminescent Homoleptic Europium Chelates. *Inorg. Chem.* **2009**, *48*, 5611−5613.

(12) Hirai, Y.; Nakanishi, T.; Kitagawa, Y.; Fushimi, K.; Seki, T.; Ito, H.; Fueno, H.; Tanaka, K.; Satoh, T.; Hasegawa, Y. Luminescent Coordination Glass: Remarkable Morphological Strategy for Assembled Eu(III) Complexes. *Inorg. Chem.* **2015**, *54*, 4364−4370.

(13) de Bettencourt-Dias, A.; Barber, P. S.; Bauer, S. A Water-Soluble Pybox Derivative and Its Highly Luminescent Lanthanide Ion Complexes. *J. Am. Chem. Soc.* **2012**, *134*, 6987−6994.

(14) D'Aléo, A.; Picot, A.; Beeby, A.; Gareth Williams, J. A.; Le Guennic, B.; Andraud, C.; Maury, O. Efficient Sensitization of Europium, Ytterbium, and Neodymium Functionalized Tris-Dipicolinate Lanthanide Complexes through Tunable Charge-Transfer Excited States. *Inorg. Chem.* **2008**, *47*, 10258−10268.

(15) Comby, S.; Imbert, D.; Chauvin, A.-S.; Bünzli, J.-C. G.; Charbonnière, L. J.; Ziessel, R. F. Influence of Anionic Functions on the Coordination and Photophysical Properties of Lanthanide(III) Complexes with Tridentate Bipyridines. *Inorg. Chem.* **2004**, *43*, 7369−7379.

(16) Shavaleev, N. M.; Eliseeva, S. V.; Scopelliti, R.; Bünzli, J.-C. G. Tridentate Benzimidazole-Pyridine-Tetrazolates as Sensitizers of Europium Luminescence. *Inorg. Chem.* **2014**, *53*, 5171−5178.

(17) Shavaleev, N. M.; Scopelliti, R.; Gumy, F.; Bünzli, J.-C. G. Benzothiazole- and Benzoxazole-Substituted Pyridine-2-Carboxylates as Efficient Sensitizers of Europium Luminescence. *Inorg. Chem.* **2009**, *48*, 6178−6191.

(18) Petoud, S.; Cohen, S. M.; Bünzli, J.-C. G.; Raymond, K. N. Stable Lanthanide Luminescence Agents Highly Emissive in Aqueous Solution: Multidentate 2-Hydroxyisophthalamide Complexes of Sm^{3+}, Eu^{3+}, Tb^{3+}, Dy^{3+}. *J. Am. Chem. Soc.* **2003**, *125*, 13324−13325.

(19) Wei, C.; Sun, B. X.; Cai, Z. L.; Zhao, Z. F.; Tan, Y.; Yan, W. B.; Wei, H. B.; Liu, Z. W.; Bian, Z. Q.; Huang, C. H. Quantum Yields over 80% Achieved in Luminescent Europium Complexes by Employing Diphenylphosphoryl Tridentate Ligands. *Inorg. Chem.* **2018**, *57*, 7512−7515.

(20) Zhao, Y.-L.; Wu, G.-J.; Li, Y.; Gao, L.-X.; Han, F.-S. $[NiCl_2(dppp)]$-Catalyzed Cross-Coupling of Aryl Halides with

Dialkyl Phosphite, Diphenylphosphine Oxide, and Diphenylphosphine. *Chem. - Eur. J.* **2012**, *18*, 9622−9627.
(21) Ruiz-Martinez, A.; Casanova, D.; Alvarez, S. Polyhedral structures with an odd number of vertices: nine-atom clusters and supramolecular architectures. *Dalton Trans.* **2008**, 2583−2591.
(22) Pinsky, M.; Avnir, D. Continuous Symmetry Measures. 5. The Classical Polyhedra. *Inorg. Chem.* **1998**, *37*, 5575−5582.
(23) (a) Shavaleev, N. M.; Eliseeva, S. V.; Scopelliti, R.; Bünzli, J.-C. G. Influence of Symmetry on the Luminescence and Radiative Lifetime of Nine-Coordinate Europium Complexes. *Inorg. Chem.* **2015**, *54*, 9166−9173. (b) Wei, C.; Wei, H.; Yan, W.; Zhao, Z.; Cai, Z.; Sun, B.; Meng, Z.; Liu, Z.; Bian, Z.; Huang, C. Water-Soluble and Highly Luminescent Europium(III) Complexes with Favorable Photostability and Sensitive pH Response Behavior. *Inorg. Chem.* **2016**, *55*, 10645−10653.
(24) Nishio, M. CH/π hydrogen bonds in crystals. *CrystEngComm* **2004**, *6*, 130−158.
(25) Spek, A. L. PLATON SQUEEZE: a tool for the calculation of the disordered solvent contribution to the calculated structure factors. *Acta Crystallogr., Sect. C: Struct. Chem.* **2015**, *71*, 9−18.
(26) (a) Binnemans, K. Interpretation of europium(III) spectra. *Coord. Chem. Rev.* **2015**, *295*, 1−45. (b) Yu, G.; Xing, Y.; Chen, F.; Han, R.; Wang, J.; Bian, Z.; Fu, L.; Liu, Z.; Ai, X.; Zhang, J.; Huang, C. Energy-Transfer Mechanisms in Ir^{III}−Eu^{III} Bimetallic Complexes. *ChemPlusChem* **2013**, *78*, 852−859.
(27) Feng, J.; Zhou, L.; Song, S.-Y.; Li, Z.-F.; Fan, W.-Q.; Sun, L.-N.; Yu, Y.-N.; Zhang, H.-J. A study on the near-infrared luminescent properties of xerogel materials doped with dysprosium complexes. *Dalton Trans.* **2009**, 6593−6598.
(28) Walton, J. W.; Carr, R.; Evans, N. H.; Funk, A. M.; Kenwright, A. M.; Parker, D.; Yufit, D. S.; Botta, M.; De Pinto, S.; Wong, K.-L. Isostructural Series of Nine-Coordinate Chiral Lanthanide Complexes Based on Triazacyclononane. *Inorg. Chem.* **2012**, *51*, 8042−8056.
(29) (a) Artizzu, F.; Mercuri, M. L.; Serpe, A.; Deplano, P. NIR-emissive erbium−quinolinolate complexes. *Coord. Chem. Rev.* **2011**, *255*, 2514−2529. (b) Monguzzi, A.; Milani, A.; Lodi, L.; Trioni, M. I.; Tubino, R.; Castiglioni, C. Vibrational overtones quenching of near infrared emission in Er^{3+} complexes. *New J. Chem.* **2009**, *33*, 1542−1548.
(30) Wei, H.; Zhao, Z.; Wei, C.; Yu, G.; Liu, Z.; Zhang, B.; Bian, J.; Bian, Z.; Huang, C. Antiphotobleaching: A Type of Structurally Rigid Chromophore Ready for Constructing Highly Luminescent and Highly Photostable Europium Complexes. *Adv. Funct. Mater.* **2016**, *26*, 2085−2096.
(31) (a) Wang, Z.; Liu, N.; Li, H.; Chen, P.; Yan, P. The Role of Blue-Emissive 1,8-Naphthalimidopyridine N-Oxide in Sensitizing Eu^{III} Photoluminescence in Dimeric Hexafluoroacetylacetonate Complexes. *Eur. J. Inorg. Chem.* **2017**, *2017*, 2211−2219. (b) Hasegawa, Y.; Tateno, S.; Yamamoto, M.; Nakanishi, T.; Kitagawa, Y.; Seki, T.; Ito, H.; Fushimi, K. Effective Photo- and Triboluminescent Europium(III) Coordination Polymers with Rigid Triangular Spacer Ligands. *Chem. - Eur. J.* **2017**, *23*, 2666−2672. (c) Freund, C.; Porzio, W.; Giovanella, U.; Vignali, F.; Pasini, M.; Destri, S.; Mech, A.; Di Pietro, S.; Di Bari, L.; Mineo, P. Thiophene Based Europium β-Diketonate Complexes: Effect of the Ligand Structure on the Emission Quantum Yield. *Inorg. Chem.* **2011**, *50*, 5417−5429. (d) Raj, D. B. A.; Biju, S.; Reddy, M. L. P. One-, Two-, and Three-Dimensional Arrays of Eu^{3+}-4,4,5,5,5-pentafluoro-1-(naphthalen-2-yl)pentane-1,3-dione complexes: Synthesis, Crystal Structure and Photophysical Properties. *Inorg. Chem.* **2008**, *47*, 8091−8100.
(32) (a) Glover, P. B.; Bassett, A. P.; Nockemann, P.; Kariuki, B. M.; Van Deun, R.; Pikramenou, Z. Fully Fluorinated Imidodiphosphinate Shells for Visible- and NIR-Emitting Lanthanides: Hitherto Unexpected Effects of Sensitizer Fluorination on Lanthanide Emission Properties. *Chem. - Eur. J.* **2007**, *13*, 6308−6320. (b) Biju, S.; Gopakumar, N.; Bünzli, J. C. G.; Scopelliti, R.; Kim, H. K.; Reddy, M. L. P. Brilliant Photoluminescence and Triboluminescence from Ternary Complexes of Dy^{III} and Tb^{III} with 3-Phenyl-4-propanoyl-5-isoxazolonate and a Bidentate Phosphine Oxide Coligand. *Inorg. Chem.* **2013**, *52*, 8750−8758. (c) Quici, S.; Cavazzini, M.; Marzanni, G.; Accorsi, G.; Armaroli, N.; Ventura, B.; Barigelletti, F. Visible and Near-Infrared Intense Luminescence from Water-Soluble Lanthanide [Tb(III), Eu(III), Sm(III), Dy(III), Pr(III), Ho(III), Yb(III), Nd(III), Er(III)] Complexes. *Inorg. Chem.* **2005**, *44*, 529−537.
(33) (a) Foucault-Collet, A.; Shade, C. M.; Nazarenko, I.; Petoud, S.; Eliseeva, S. V. Polynuclear Sm^{III} Polyamidoamine-Based Dendrimer: A Single Probe for Combined Visible and Near-Infrared Live-Cell Imaging. *Angew. Chem., Int. Ed.* **2014**, *53*, 2927−2930. (b) Lo, W.-S.; Zhang, J.; Wong, W.-T.; Law, G.-L. Highly Luminescent SmIII Complexes with Intraligand Charge-Transfer Sensitization and the Effect of Solvent Polarity on Their Luminescent Properties. *Inorg. Chem.* **2015**, *54*, 3725−3727. (c) Biju, S.; Eom, Y. K.; Bunzli, J.-C. G.; Kim, H. K. A new tetrakis β-diketone ligand for NIR emitting Ln^{III} ions: luminescent doped PMMA films and flexible resins for advanced photonic applications. *J. Mater. Chem. C* **2013**, *1*, 6935−6944.
(34) Sager, W. F.; Filipescu, N.; Serafin, F. A. Substituent Effects on Intramolecular Energy Transfer. I. Absorption and Phosphorescence Spectra of Rare Earth β-Diketone Chelates. *J. Phys. Chem.* **1965**, *69*, 1092−1100.
(35) Biju, S.; Freire, R. O.; Eom, Y. K.; Scopelliti, R.; Bünzli, J.-C. G.; Kim, H. K. A Eu^{III} Tetrakis(β-diketonate) Dimeric Complex: Photophysical Properties, Structural Elucidation by Sparkle/AM1 Calculations, and Doping into PMMA Films and Nanowires. *Inorg. Chem.* **2014**, *53*, 8407−8417.
(36) Latva, M.; Takalo, H.; Mukkala, V.-M.; Matachescu, C.; Rodríguez-Ubis, J. C.; Kankare, J. Correlation between the lowest triplet state energy level of the ligand and lanthanide(III) luminescence quantum yield. *J. Lumin.* **1997**, *75*, 149−169.
(37) Yang, C.; Fu, L.-M.; Wang, Y.; Zhang, J.-P.; Wong, W.-T.; Ai, X.-C.; Qiao, Y.-F.; Zou, B.-S.; Gui, L.-L. A Highly Luminescent Europium Complex Showing Visible-Light-Sensitized Red Emission: Direct Observation of the Singlet Pathway. *Angew. Chem.* **2004**, *116*, 5120−5123.
(38) Murphy, C. B.; Zhang, Y.; Troxler, T.; Ferry, V.; Martin, J. J.; Jones, W. E. Probing Förster and Dexter Energy-Transfer Mechanisms in Fluorescent Conjugated Polymer Chemosensors. *J. Phys. Chem. B* **2004**, *108*, 1537−1543.
(39) (a) Carnall, W. T.; Fields, P. R.; Rajnak, K. Electronic Energy Levels in the Trivalent Lanthanide Aquo Ions. I. Pr^{3+}, Nd^{3+}, Pm^{3+}, Sm^{3+}, Dy^{3+}, Ho^{3+}, Er^{3+}, and Tm^{3+}. *J. Chem. Phys.* **1968**, *49*, 4424−4442. (b) Carnall, W. T.; Fields, P. R.; Rajnak, K. Electronic Energy Levels of the Trivalent Lanthanide Aquo Ions. III. Tb^{3+}. *J. Chem. Phys.* **1968**, *49*, 4447−4449. (c) Carnall, W. T.; Fields, P. R.; Rajnak, K. Electronic Energy Levels of the Trivalent Lanthanide Aquo Ions. IV. Eu^{3+}. *J. Chem. Phys.* **1968**, *49*, 4450−4455.
(40) Steemers, F. J.; Verboom, W.; Reinhoudt, D. N.; van der Tol, E. B.; Verhoeven, J. W. New Sensitizer-Modified Calix[4]arenes Enabling Near-UV Excitation of Complexed Luminescent Lanthanide Ions. *J. Am. Chem. Soc.* **1995**, *117*, 9408−9414.
(41) Wei, H.; Yu, G.; Zhao, Z.; Liu, Z.; Bian, Z.; Huang, C. Constructing lanthanide [Nd(iii), Er(iii) and Yb(iii)] complexes using a tridentate N, N, O-ligand for near-infrared organic light-emitting diodes. *Dalton Trans.* **2013**, *42*, 8951−8960.
(42) (a) Klink, S. I.; Hebbink, G. A.; Grave, L.; Oude Alink, P. G. B.; van Veggel, F. C. J. M.; Werts, M. H. V. Synergistic Complexation of Eu^{3+} by a Polydentate Ligand and a Bidentate Antenna to Obtain Ternary Complexes with High Luminescence Quantum Yields. *J. Phys. Chem. A* **2002**, *106*, 3681−3689. (b) Werts, M. H. V.; Jukes, R. T. F.; Verhoeven, J. W. The emission spectrum and the radiative lifetime of Eu^{3+} in luminescent lanthanide complexes. *Phys. Chem. Chem. Phys.* **2002**, *4*, 1542−1548.

https://dx.doi.org/10.1021/acs.inorgchem.0c00444
Inorg. Chem. XXXX, XXX, XXX−XXX